

Jun Lei*, Pengbo Sun, and Tinh Quoc Bui

Determination of fracture parameters for interface cracks in transverse isotropic magneto-electroelastic composites

Abstract: To determine fracture parameters of interfacial cracks in transverse isotropic magneto-electroelastic composites, a displacement extrapolation formula was derived. The matrix-form formula can be applicable for both material components with arbitrary poling directions. The corresponding explicit expression of this formula was obtained for each poling direction normal to the crack plane. This displacement extrapolation formula is only related to the boundary quantities of the extended crack opening displacements across crack faces, which is convenient for numerical applications, especially for BEM. Meantime, an alternative extrapolation formula based on the path-independent J-integral and displacement ratios was presented which may be more adaptable for any domain-based numerical techniques like FEM. A numerical example was presented to show the correctness of these formulae.

Keywords: displacement extrapolation formula; fracture parameters; magneto-electroelastic; interfacial crack; J integral

DOI 10.1515/cls-2015-0014

Received January 2, 2015; accepted January 30, 2015

1 Introduction

Magneto-electroelastic (MEE) composites usually consist of piezoelectric and piezomagnetic phases. A unique magneto-electric coupling effect will behave but absent in each

constitute [1], which even a hundred times larger than that in a single phase [2]. The special ability of energy conversion among mechanical, electric and magnetic fields leads MEE materials to increasingly extensive applications in multifunctional devices, such as electromagnetic transducers, sensors and actuators in recent years. Many efforts are focused on modeling the coupling effects [3, 4] or free vibrations of MEE plates [5–7]. But unfortunately, MEE composites are inherently brittle and inclined to cracking. This will definitely influence the behavior of the composites and the life time of these devices. So it is of very importance to study the fracture mechanics of MEE materials.


The solutions to various crack problems in MEE composites have been proposed. For example, Wang and Mai [8] derived the expression of the crack-tip asymptotic fields. Most existing works are dealt with cracks in a homogeneous media, e.g. [9, 10] for anti-plane problems, [11–14] for in-plane crack problems and [15, 16] for penny-shape crack problems, respectively. As known to us, the laminated composite structures are often used to enhance the coupling effects in multilayer actuators. The interface debonding plays a principal role on the failure of the layered MEE structures. However, the interfacial cracks between different MEE phases are rarely considered. Most works are related to anti-plane deformations [17–20]. The transient response of an interfacial crack between dissimilar MEE layers under in-plane magneto-electromechanical impacts was analyzed by [21].

For the limitation of these analytical methods for simple crack problems, numerical methods are irreplaceable to deal with more general cases. Although a variety of numerical methods has been developed for dealing with static or dynamic fracture problems in MEE composites [22–26], to authors' knowledge, few published literatures about numerical treatments with MEE interfacial crack problems can be referred. This is due to the lack of a simple and easy extrapolating formula for determination of the fracture parameters for these interfacial cracks. To this end, a displacement extrapolating formula for numerical applications will be derived in this pa-

*Corresponding Author: Jun Lei: Department of Engineering Mechanics, Beijing University of Technology, Beijing 100124, PR China, E-mail: lejun@bjut.edu.cn; Tel: ++86-15810850418

Pengbo Sun: Department of Engineering Mechanics, Beijing University of Technology, Beijing 100124, PR China

Tinh Quoc Bui: Department of Mechanical and Environmental Informatics, Tokyo Institute of Technology, 2-12-1-W8-22, Ookayama, Meguro-ku, Tokyo 152-8552, Japan

 © 2015 Jun Lei et al., licensee De Gruyter Open.

This work is licensed under the Creative Commons Attribution-NonCommercial-NoDerivs 3.0 License.

per. The relations between the extended crack opening displacements (ECODs) and the field intensity factors of an interfacial crack are obtained by means of the crack-tip asymptotic fields [27]. To avoid solving the emerging complex eigen equations, a matrix-form extrapolating formula for transversely isotropic MEE bi-materials with arbitrary poling directions is derived by using the expressions in [28, 29]. The corresponding explicit extrapolating formula for both poling directions perpendicular to crack plane is also presented. Further, on the basis of a path-independent J-integral and the crack-face displacement ratios, an alternative extrapolation formula is deduced which may be more adaptable for any domain-based numerical techniques like FEM or XFEM [30–32]. Finally, a numerical example is presented to verify these formulae.

2 Basic equations for magneto-electroelastic materials

Consider in-plane deformations of a homogeneous and fully anisotropic magneto-electro-elastic material which possess linear coupling between stress, electric field and magnetic field. Thus, the constitutive relations are:

$$\begin{cases} \sigma_{ij} = c_{ijkl}\varepsilon_{kl} - e_{lij}E_l - h_{lij}H_l \\ D_i = e_{ikl}\varepsilon_{kl} + \kappa_{il}E_l + \beta_{il}H_l \\ B_i = h_{ikl}\varepsilon_{kl} + \beta_{il}E_l + \gamma_{il}H_l \end{cases}, \quad (1)$$

where σ_{ij} and ε_{ij} are the components of mechanical stress and strain; D_i and E_i the components of electric displacement and field; B_i and H_i magnetic induction and field, respectively; c_{ijkl} , κ_{ik} and γ_{il} are the elastic stiffness tensor, the dielectric permittivity tensor and the magnetic permeability tensor; e_{kij} , h_{lij} and β_{il} are the piezoelectric, piezomagnetic and magnetoelectric coupling coefficients. The following reciprocal symmetries hold

$$\begin{cases} c_{ijkl} = c_{jikl} = c_{ijlk} = c_{lkji}, & e_{kij} = e_{kji} \\ h_{kij} = h_{kji}, & \kappa_{ij} = \kappa_{ji}, \beta_{ij} = \beta_{ji}, \gamma_{ij} = \gamma_{ji} \end{cases}. \quad (2)$$

The strain ε_{ij} , electric field E_i and magnetic field H_i can be related to displacements u_i , electric potential ϕ and magnetic potential φ via the following divergence and gradient equations

$$\varepsilon_{ij} = \frac{1}{2}(u_{i,j} + u_{j,i}), \quad E_i = -\phi_{,i}, \quad H_i = -\varphi_{,i}. \quad (3)$$

In the absence of body forces, electric charge and current densities, the equilibrium equations can be written as

$$\sigma_{ij,j} = 0, \quad D_{i,i} = 0, \quad B_{i,i} = 0. \quad (4)$$

For convenience, the following generalized displacement vector u_J , stress tensor σ_{ij} , strain tensor ε_{ij} , and the generalized elasticity tensor c_{ijkl} are introduced

$$u_J = [u_i, \phi, \varphi]^T, \quad \sigma_{ij} = [\sigma_{ij}, D_i, B_i], \quad \varepsilon_{ij} = [\varepsilon_{ij}, -E_i, -H_i], \quad (5)$$

$$c_{ijkl} \equiv \begin{cases} c_{ijkl} = c_{ijkl}, & J, K = 1, 2 \\ c_{ij3l} = e_{lij}, c_{i3kl} = e_{ikl}, c_{ij4l} = h_{lij}, c_{i4kl} = h_{ikl} \\ c_{i33l} = -\kappa_{il}, c_{i34l} = -\beta_{il}, c_{i43l} = -\beta_{il}, c_{i44l} = -\gamma_{il} \end{cases} \quad (6)$$

where the lowercase and uppercase subscripts take values 1, 2 and 1-4, respectively.

3 Crack-tip fields for an interfacial crack

Considering an asymptotic problem of an interfacial crack of a length $2a$ lies on the interface $x_2 = 0$ between two half spaces, see Fig. 1, material I above, and II below. The singular crack-tip fields of this model under remote loadings $\mathbf{t}_2^0 = [\sigma_{22}^\infty, D_2^\infty, B_2^\infty]^T$ can be solved by an equivalent cracked system with $-\mathbf{t}_2^0$ acting on the crack surface. Then the continuity and boundary conditions along $x_2 = 0$ can be written as

$$\mathbf{t}_2^I(x_1) = \mathbf{t}_2^{II}(x_1), \quad |x_1| < \infty, \quad (7)$$

$$\mathbf{t}_2^I(x_1) = \mathbf{t}_2^{II}(x_1) = -\mathbf{t}_2^0, \quad |x_1| \leq a, \quad (8)$$

$$u_J^I(x_1) = u_J^{II}(x_1), \quad |x_1| \geq a, \quad (9)$$

with the superscript I and II denote the upper and lower medium, respectively.

The solution to this interfacial crack problem has been derived by Huang et al. [27]. Accordingly, the crack-tip asymptotic fields related to the generalized field intensity factors \mathbf{K} are directly presented here

$$\delta(r) = (\mathbf{H} + \bar{\mathbf{H}}) \sqrt{\frac{r}{2\pi}} \sum_{j=1}^4 \frac{K_j r^{i\lambda_j} \mathbf{w}_j}{(1 + 2i\lambda_j) \cosh \pi\lambda_j}, \quad (10)$$

in which the extended crack opening displacements (ECODs) $\delta = [\Delta u_1, \Delta u_3, \Delta \phi, \Delta \varphi]^T$ include the crack opening displacements, electric and magnetic potential jumps. The components of $\mathbf{K} = [K_1, K_2, K_3, K_4]^T$ one to one correspond to the mode-II intensity factor K_{II} , mode-I K_I , electric displacement intensity factor K_D and magnetic induction intensity factor K_B . \mathbf{H} is a bi-material matrix defined as

$$\mathbf{H} = \mathbf{Y}_I + \bar{\mathbf{Y}}_{II}, \quad (11)$$

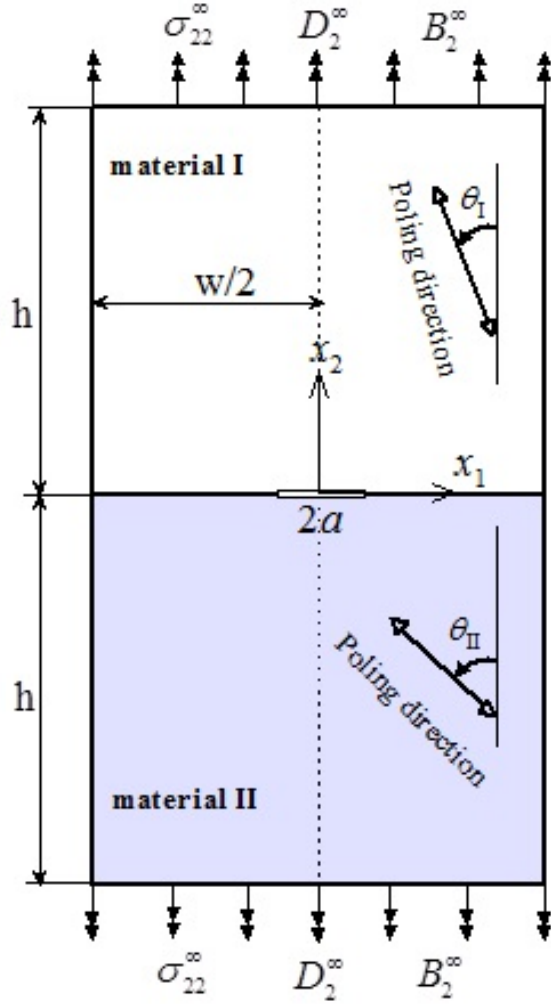


Figure 1: A central interfacial crack in a MEE bi-material.

with $\mathbf{Y} = i\mathbf{A}\mathbf{B}^{-1}$ being the well-known Irwin matrix which can be referred to Lei et al. [29]; \mathbf{w}_j is the eigenvector of the following eigenvalue problem

$$\bar{\mathbf{H}}\mathbf{w}_j = e^{2\pi\lambda} \mathbf{H}\mathbf{w}_j, \tag{12}$$

and the parameter λ_j satisfies

$$\det [\bar{\mathbf{H}} - e^{2\pi\lambda} \mathbf{H}] = 0. \tag{13}$$

Since \mathbf{H} is Hermitian, if λ satisfies equation 13, so do $-\lambda$, $\bar{\lambda}$ and $-\bar{\lambda}$.

It should be noted that the equation 11 or 14 can be directly adopted as displacement extrapolation formulae for numerical methods to determinate the field intensity factors of an interfacial crack in any fully anisotropic MEE materials. But the complex characteristic equations 13 should be carefully treated. The relation 10 can be further rewrit-

ten in the following form [28]

$$\delta = \frac{4\sqrt{r}}{\sqrt{2\pi}} \mathbf{H}\Lambda \left\langle \frac{r^{i\lambda_j} \cosh\pi\lambda_j}{1 + 2i\lambda_j} \right\rangle \Lambda^{-1} (\mathbf{I} + \bar{\mathbf{H}}^{-1}\mathbf{H})^{-1} \mathbf{K}, \tag{14}$$

with $\Lambda = [\mathbf{w}_1, \mathbf{w}_2, \mathbf{w}_3, \mathbf{w}_4]$ and the symbol $\langle \rangle$ denotes a diagonal matrix.

4 The displacement extrapolation formula

4.1 The matrix-form displacement extrapolation formulae

Without loss of generality, only transverse isotropic MEE materials are considered here because most of them possess transverse isotropic. For a transverse isotropic MEE material, the explicit expression of the Irwin matrix \mathbf{Y} has been deduced using an extended Lekhnitskii formalism by Lei et al. [29]. Then letting $\mathbf{H} = \mathbf{V} + i\mathbf{F}$ and $\mathbf{E} = \mathbf{V}^{-1}\mathbf{F}$, the bi-material matrix $\mathbf{H} = \mathbf{V} + i\mathbf{F}$ takes the following form [29]

$$\mathbf{V} = \begin{bmatrix} v_{11} & 0 & 0 & 0 \\ 0 & v_{22} & v_{23} & v_{24} \\ 0 & v_{23} & v_{33} & v_{34} \\ 0 & v_{24} & v_{34} & v_{44} \end{bmatrix}, \tag{15}$$

$$\mathbf{F} = \begin{bmatrix} 0 & f_{12} & f_{13} & f_{14} \\ -f_{12} & 0 & 0 & 0 \\ -f_{13} & 0 & 0 & 0 \\ -f_{14} & 0 & 0 & 0 \end{bmatrix},$$

for the poling axis perpendicular to the crack plane. Because of the sparse and antisymmetric structure, the rank of the matrix \mathbf{F} is just two. So the following equation will be always valid

$$c = \det[\mathbf{E}] = \det[\mathbf{V}^{-1}] \cdot \det[\mathbf{F}] = 0 \quad (\det[\mathbf{F}] = 0). \tag{16}$$

Further consider a more general case that the two poling axes of material I and II are rotated at any different angles to the Cartesian coordinate axes. The following work is to prove the validation of $\det[\mathbf{E}] = 0$ under any in-plane coordinate rotations.

Assume the two in-plane coordinate rotations are about x_3 -axis with angle θ_I and θ_{II} which denote the rotation angle from x to the new coordinate axis x^* , as shown in Fig. 1. The corresponding transformation matrices take the form

$$\mathfrak{R}_i = \begin{bmatrix} \cos \theta_i & \sin \theta_i & 0 & 0 \\ -\sin \theta_i & \cos \theta_i & 0 & 0 \\ 0 & 0 & 1 & 0 \\ 0 & 0 & 0 & 1 \end{bmatrix}, \quad i = \text{I, II}. \tag{17}$$

Given the Irwin matrix $\mathbf{Y}_I = \mathbf{V}_1 + i\mathbf{F}_1$ and $\mathbf{Y}_{II} = \mathbf{V}_2 + i\mathbf{F}_2$. Obviously, the structures of \mathbf{V}_i and \mathbf{F}_i are the same as the expression 15. After the coordinate rotation \mathfrak{R}_I and \mathfrak{R}_{II} , the rotated $\widehat{\mathbf{H}} = \widehat{\mathbf{V}} + i\widehat{\mathbf{F}}$ can be expressed as

$$\begin{cases} \widehat{\mathbf{V}} = \widehat{\mathbf{V}}_1 + \widehat{\mathbf{V}}_2 = \mathfrak{R}_I \mathbf{V}_1 \mathfrak{R}_I^T + \mathfrak{R}_{II} \mathbf{V}_2 \mathfrak{R}_{II}^T \\ \widehat{\mathbf{F}} = \widehat{\mathbf{F}}_1 - \widehat{\mathbf{F}}_2 = \mathfrak{R}_I \mathbf{F}_1 \mathfrak{R}_I^T - \mathfrak{R}_{II} \mathbf{F}_2 \mathfrak{R}_{II}^T \end{cases}, \quad (18)$$

here $\widehat{\mathbf{F}}$ is still a sparse and antisymmetric structure and takes the form

$$\widehat{\mathbf{F}} = \begin{bmatrix} 0 & \widehat{f}_{12} & \widehat{f}_{13} & \widehat{f}_{14} \\ -\widehat{f}_{12} & 0 & -\widehat{f}_{13} & -\widehat{f}_{14} \\ -\widehat{f}_{13} & \widehat{f}_{13} & 0 & 0 \\ -\widehat{f}_{14} & \widehat{f}_{14} & 0 & 0 \end{bmatrix}, \quad (19)$$

with $\det[\widehat{\mathbf{F}}] = 0$. Then the determination of the rotated $\widehat{\mathbf{E}}$ still equal to zero, i.e., $\det[\widehat{\mathbf{E}}] = \det[\widehat{\mathbf{V}}^{-1}] \cdot \det[\widehat{\mathbf{F}}] = 0$.

By means of $\mathbf{H} = \mathbf{V} + i\mathbf{F}$ and $\mathbf{E} = \mathbf{V}^{-1}\mathbf{F}$, the eigen equation 12 can be written as

$$(\mathbf{E} + i\beta\mathbf{I})\mathbf{w} = 0, \quad (20)$$

with

$$\beta = -\tanh(\pi\lambda) \text{ or } \lambda = \frac{1}{2\pi} \ln \frac{1-\beta}{1+\beta}. \quad (21)$$

Observed from the relation between β and λ , β accompanied with $-\beta$, $\bar{\beta}$ and $-\bar{\beta}$ will all satisfy the equation 20, its characteristic equation can have a simple form

$$\det[\mathbf{E} + i\beta\mathbf{I}] = \beta^4 + 2b\beta^2 + c = 0, \quad (22)$$

in which $b = \frac{1}{4}\text{tr}[\mathbf{E}^2]$, $c = \det[\mathbf{E}]$ and $\text{tr}[\]$ stands for the trace of a matrix.

Due to $\det[\widehat{\mathbf{E}}] = 0$ as mentioned above, the roots of Eq. 22 can be expressed as

$$\beta_{1,2} = \pm\sqrt{-2b}, \quad \beta_{3,4} = 0. \quad (23)$$

Then the oscillatory singularity of the crack-tip field can be imaginary or real, which just depends on the sign of $b = \text{tr}[\mathbf{E}^2]/4$. The four eigenpairs $((\lambda_j, \mathbf{w}_j))$ have the following structures

$$\begin{cases} (\varepsilon, \mathbf{w}_1), (-\varepsilon, \bar{\mathbf{w}}_1), (0, \mathbf{w}_3), (0, \mathbf{w}_4), \\ \quad \varepsilon = \frac{1}{2\pi} \ln \frac{1-\beta}{1+\beta} \text{ for } b < 0 \\ (-i\kappa, \mathbf{w}_1), (i\kappa, \mathbf{w}_2), (0, \mathbf{w}_3), (0, \mathbf{w}_4), \\ \quad \kappa = \frac{1}{2\pi i} \ln \frac{1-\beta}{1+\beta} \text{ for } b > 0 \end{cases}. \quad (24)$$

Based on these solutions, the relations 14 can be written as

$$\delta = \frac{4\sqrt{r}}{\sqrt{2\pi}} \mathbf{H}\Lambda \langle \xi_1, \xi_2, 1, 1 \rangle \Lambda^{-1} (\mathbf{I} + \bar{\mathbf{H}}^{-1}\mathbf{H})^{-1} \mathbf{K}, \quad (25)$$

in which

$$\xi_1 = \begin{cases} r^{ie} \frac{\cosh \pi\varepsilon}{1+2i\varepsilon}, & b < 0 \\ r^\kappa \frac{\cos \pi\kappa}{1+2\kappa}, & b > 0 \end{cases}, \quad (26)$$

$$\xi_2 = \begin{cases} r^{-ie} \frac{\cosh \pi\varepsilon}{1-2i\varepsilon} = \bar{\xi}_1, & b < 0 \\ r^{-\kappa} \frac{\cos \pi\kappa}{1-2\kappa}, & b > 0 \end{cases}.$$

Introduce the following expression 28

$$\Lambda \langle \mu_j \rangle \Lambda^{-1} = \mathbf{G}_1\mu_1 + \mathbf{G}_2\mu_2 + \mathbf{G}_3\mu_3 + \mathbf{G}_4\mu_4, \quad (27)$$

the relation 25 can be further rewritten as

$$\delta = \frac{4\sqrt{r}}{\sqrt{2\pi}} \mathbf{H}[\mathbf{G}_1\xi_1 + \mathbf{G}_2\xi_2 + \mathbf{G}_3 + \mathbf{G}_4] (\mathbf{I} + \bar{\mathbf{H}}^{-1}\mathbf{H})^{-1} \mathbf{K}. \quad (28)$$

First consider the case of $\text{tr}[\mathbf{E}^2] < 0$, the oscillatory singularity ε is imaginary with $\beta = -\sqrt{-2b}$ in this case. The associated eigenvectors will satisfy

$$\mathbf{E}\mathbf{w}_1 = -i\beta\mathbf{w}_1, \quad \mathbf{E}\bar{\mathbf{w}}_1 = i\beta\bar{\mathbf{w}}_1, \quad \mathbf{E}\mathbf{w}_3 = 0, \quad \mathbf{E}\mathbf{w}_4 = 0. \quad (29)$$

Considering the properties of Λ given in Eq. 27, the following matrix equation system of \mathbf{G}_i can be obtained after algebraic operations

$$\begin{cases} \mathbf{G}_1 + \mathbf{G}_2 + \mathbf{G}_3 + \mathbf{G}_4 = \mathbf{I} \\ -i\beta\mathbf{G}_1\Lambda + i\beta\mathbf{G}_2\Lambda = \mathbf{E}\Lambda \\ -\beta^2\mathbf{G}_1\Lambda - \beta^2\mathbf{G}_2\Lambda = \mathbf{E}^2\Lambda \end{cases}. \quad (30)$$

By using the elimination method, \mathbf{G}_i can be achieved

$$\begin{cases} \mathbf{G}_1 = -\frac{1}{2\beta^2} (\mathbf{E}^2 - i\beta\mathbf{E}) \\ \mathbf{G}_2 = -\frac{1}{2\beta^2} (\mathbf{E}^2 + i\beta\mathbf{E}) = \bar{\mathbf{G}}_1 \\ \mathbf{G}_3 + \mathbf{G}_4 = \frac{1}{\beta^2} (\mathbf{E}^2 + \beta^2\mathbf{I}) \end{cases}. \quad (31)$$

Then the relations 28 can be given as

$$\mathbf{K} = \sqrt{\frac{\pi}{2r}} \left\{ [1 - \text{Re}(\xi_1)] \frac{1}{\beta^2} \mathbf{T}_3 - \text{Im}(\xi_1) \frac{1}{\beta} \mathbf{T}_2 + \mathbf{T}_1 \right\}^{-1} \delta, \quad (32)$$

with

$$\begin{cases} \mathbf{T}_1 = 2\mathbf{H}(\mathbf{I} + \bar{\mathbf{H}}^{-1}\mathbf{H})^{-1} \\ \mathbf{T}_2 = 2\mathbf{H}\mathbf{E}(\mathbf{I} + \bar{\mathbf{H}}^{-1}\mathbf{H})^{-1} \\ \mathbf{T}_3 = 2\mathbf{H}\mathbf{E}^2(\mathbf{I} + \bar{\mathbf{H}}^{-1}\mathbf{H})^{-1} \end{cases}. \quad (33)$$

In the same way, the case of $\text{tr}[\mathbf{E}^2] > 0$ is analyzed for the real oscillatory singularity κ and $\beta = -\sqrt{2b}$. In this condition, the associated eigenvectors satisfy

$$\mathbf{E}\mathbf{w}_1 = \beta\mathbf{w}_1, \quad \mathbf{E}\mathbf{w}_2 = -\beta\mathbf{w}_2, \quad \mathbf{E}\mathbf{w}_3 = 0, \quad \mathbf{E}\mathbf{w}_4 = 0, \quad (34)$$

and the expressions of \mathbf{G}_i can be easily obtained as

$$\begin{cases} \mathbf{G}_1 = \frac{1}{2\beta^2} (\mathbf{E}^2 + \beta\mathbf{E}) \\ \mathbf{G}_2 = \frac{1}{2\beta^2} (\mathbf{E}^2 - \beta\mathbf{E}) \\ \mathbf{G}_3 + \mathbf{G}_4 = \frac{-1}{\beta^2} (\mathbf{E}^2 - \beta^2\mathbf{I}) \end{cases}. \quad (35)$$

Then the relations between \mathbf{K} and ECODs can be expressed as

$$\mathbf{K} = \sqrt{\frac{\pi}{2r}} \left\{ \left[\frac{1}{2}(\xi_1 + \xi_2) - 1 \right] \frac{1}{\beta^2} \mathbf{T}_3 + (\xi_1 - \xi_2) \frac{1}{\beta} \mathbf{T}_2 + \mathbf{T}_1 \right\}^{-1} \delta. \quad (36)$$

It should be noted that the matrix-form extrapolating formulae 32 and 36 are valid for the interfacial crack in transversely isotropic MEE composites with arbitrary poling directions.

4.2 Explicit expressions of \mathbf{T}_i

In this section, a typical case for both poling axes of the components perpendicular to the crack plane is treated. With the aid of Mathematica software using the matrix in Eq. 15, the explicit expression of matrices \mathbf{T}_i can be obtained

$$\mathbf{T}_1 = \begin{bmatrix} d_0 + v_{11} & 0 & 0 & 0 \\ 0 & d_1 & d_2 & d_3 \\ 0 & d_2 & d_4 & d_5 \\ 0 & d_3 & d_5 & d_6 \end{bmatrix}, \quad (37)$$

$$\mathbf{T}_2 = \frac{d_0 + v_{11}}{v_{11}} \begin{bmatrix} 0 & f_{12} & f_{13} & f_{14} \\ -f_{12} & 0 & 0 & 0 \\ -f_{13} & 0 & 0 & 0 \\ -f_{14} & 0 & 0 & 0 \end{bmatrix}, \quad (38)$$

$$\mathbf{T}_3 = -\frac{d_0 + v_{11}}{v_{11}^2} \begin{bmatrix} -v_{11}d_0 & 0 & 0 & 0 \\ 0 & f_{12}^2 & f_{12}f_{13} & f_{12}f_{14} \\ 0 & f_{12}f_{13} & f_{13}^2 & f_{13}f_{14} \\ 0 & f_{12}f_{14} & f_{13}f_{14} & f_{14}^2 \end{bmatrix}, \quad (39)$$

in which

$$\Delta = v_{24}^2 v_{33} + v_{23}^2 v_{44} + v_{22} v_{34}^2 - 2v_{23} v_{24} v_{34} - v_{22} v_{33} v_{44}, \quad (40)$$

$$d_0 = \frac{1}{\Delta} \left[f_{12}^2 (v_{33} v_{44} - v_{34}^2) + f_{13}^2 (v_{22} v_{44} - v_{24}^2) + f_{14}^2 (v_{22} v_{33} - v_{23}^2) + 2f_{12} f_{13} (v_{24} v_{34} - v_{23} v_{44}) + 2f_{12} f_{14} (v_{23} v_{34} - v_{24} v_{33}) + 2f_{13} f_{14} (v_{23} v_{24} - v_{22} v_{34}) \right], \quad (41)$$

$$\begin{cases} d_1 = v_{22} - f_{12}^2/v_{11}, & d_2 = v_{23} - f_{12}f_{13}/v_{11} \\ d_3 = v_{24} - f_{12}f_{14}/v_{11}, & d_4 = v_{33} - f_{13}^2/v_{11} \\ d_5 = v_{34} - f_{13}f_{14}/v_{11}, & d_6 = v_{44} - f_{14}^2/v_{11} \end{cases}. \quad (42)$$

Using the \mathbf{T}_i expressions 37, 38, 39, the extrapolation formulae 32 and 36 can be expressed in explicit forms.

5 An alternative extrapolation formulae based on J integral

It is more popular to calculate the crack-tip energy release rate (ERR) G by the path-independent J integral in finite element analyses. For a cracked MEE material, the J integral was defined as [15]

$$J_1 = G = \int_{\Gamma} (W n_1 - \sigma_{ij} n_i u_{j,1}) d\Gamma, \quad (43)$$

where Γ is an arbitrary enclosing contour around the crack tip and n_j is the outward normal vector, and $W = \sigma_{ij} \varepsilon_{ij} / 2$ is the electromagnetic enthalpy density.

The following work is how to extract the field intensity factors from ERR based on their relation [10]

$$G = \frac{1}{4} \mathbf{K}^T \mathbf{T}_1 \mathbf{K}. \quad (44)$$

Observed the structures of the coefficient matrices \mathbf{T}_i , the extrapolation formulae 32, 36 can be written in the following form

$$\mathbf{K} = \sqrt{\frac{\pi}{2r}} \begin{bmatrix} m_{11} & m_{12} & m_{13} & m_{14} \\ -m_{12} & m_{22} & m_{23} & m_{24} \\ -m_{13} & m_{23} & m_{33} & m_{34} \\ -m_{14} & m_{24} & m_{34} & m_{44} \end{bmatrix}^{-1} \delta = \sqrt{\frac{\pi}{2r}} \mathbf{M}^{-1} \delta. \quad (45)$$

By means of Eq. 37, the J-integral can be expanded as

$$J_1 = G = \frac{1}{4} \mathbf{K}^T \mathbf{T}_1 \mathbf{K} = \frac{1}{4} \left[(d_0 + v_{11}) K_1^2 + d_1 K_2^2 + d_4 K_3^2 + d_6 K_4^2 + 2d_2 K_2 K_3 + 2d_3 K_2 K_4 + 2d_5 K_3 K_4 \right], \quad (46)$$

Introduce the ratio $q_I = \delta_I / \delta_2$ and $s_I = b_{IJ} q_J$, then the field intensity factors can be extracted from the value of J-integral by

$$K_J = s_J \frac{2 \operatorname{sgn}(\det[\mathbf{M}]) \sqrt{|J_1|}}{\sqrt{|\mathbf{II}|}}, \quad (47)$$

in which $\operatorname{sgn}(\cdot)$ stands for the sign function and

$$\begin{cases} b_{11} = -m_{24}^2 m_{33} - m_{22} m_{34}^2 - m_{23}^2 m_{44} + 2m_{23} m_{24} m_{34} \\ \quad + m_{22} m_{33} m_{44} \\ b_{12} = -b_{21} = m_{14} (m_{24} m_{33} - m_{23} m_{34}) + m_{34} (m_{12} m_{34} \\ \quad - m_{13} m_{24}) + m_{44} (m_{13} m_{23} - m_{12} m_{33}) \\ b_{13} = -b_{31} = m_{24} (m_{13} m_{24} - m_{23} m_{14}) + m_{34} (m_{14} m_{22} \\ \quad - m_{12} m_{24}) + m_{44} (m_{12} m_{23} - m_{13} m_{22}) \\ b_{14} = -b_{41} = m_{24} (m_{12} m_{33} - m_{13} m_{23}) + m_{14} (m_{23}^2 \\ \quad - m_{22} m_{33}) + m_{34} (m_{13} m_{22} - m_{12} m_{23}) \end{cases}, \quad (48)$$

$$\left\{ \begin{array}{l} b_{22} = m_{14}^2 m_{33} - m_{11} m_{34}^2 + m_{13}^2 m_{44} - 2m_{13} m_{14} m_{34} \\ \quad + m_{11} m_{33} m_{44} \\ b_{23} = b_{32} = m_{14} (m_{13} m_{24} - m_{14} m_{23}) + m_{34} (m_{12} m_{14} \\ \quad + m_{11} m_{24}) - m_{44} (m_{11} m_{23} + m_{12} m_{13}) \\ b_{24} = b_{42} = m_{13} (m_{14} m_{23} - m_{13} m_{24}) - m_{33} (m_{12} m_{14} \\ \quad + m_{11} m_{24}) + m_{34} (m_{11} m_{23} + m_{12} m_{13}) \end{array} \right. , \quad (49)$$

$$\left\{ \begin{array}{l} b_{33} = m_{14}^2 m_{22} - m_{11} m_{24}^2 + m_{12}^2 m_{44} - 2m_{12} m_{14} m_{24} \\ \quad + m_{11} m_{22} m_{44} \\ b_{34} = b_{43} = m_{14} (m_{12} m_{23} - m_{13} m_{22}) + m_{24} (m_{12} m_{13} \\ \quad + m_{11} m_{23}) - m_{34} (m_{12}^2 + m_{11} m_{22}) \\ b_{44} = m_{13}^2 m_{22} - m_{11} m_{23}^2 + m_{12}^2 m_{33} - 2m_{12} m_{13} m_{23} \\ \quad + m_{11} m_{22} m_{33} \end{array} \right. , \quad (50)$$

$$\begin{aligned} \Pi = & (d_0 + v_{11})s_1^2 + d_1 s_2^2 + d_4 s_3^2 + d_6 s_4^2 + 2(d_2 s_2 s_3 \\ & + d_3 s_2 s_4 + d_5 s_3 s_4). \end{aligned} \quad (51)$$

It is desirable that the relation 47 is just related to the displacement ratios δ_I/δ_2 and the value of J-integral, which may be more efficient for numerical calculations.

6 An example for verification

In this section, a central interface crack between two bonded MEE rectangular plates is considered, see Fig. 1. The geometrical parameters are fixed as $2a = 4.8$ mm and $w = h = 20$ mm. The bi-material is under coupling loads $\mathbf{t}_2^0 = [\sigma_{22}^\infty, D_2^\infty, B_2^\infty]^T$. In the following examples, the transversely isotropic BaTiO₃-CoFe₂O₄ MEE composite materials are considered. They are made of the piezoelectric material BaTiO₃ as the inclusion and the piezomagnetic material CoFe₂O₄ as the matrix with a volume fraction of the inclusion V_f . The volume fraction of the upper material I is fixed as $V_f^I = 0.5$. The material constants of BaTiO₃ and CoFe₂O₄ are listed as follows

$$\begin{aligned} \text{BaTiO}_3 : \\ c_{11} = 166\text{GPa}, c_{13} = 78\text{GPa}, c_{33} = 162\text{GPa}, c_{44} = 43\text{GPa}, \\ e_{31} = 11.6\text{C/m}^2, e_{33} = -4.4\text{C/m}^2, e_{15} = 18.6\text{C/m}^2, \\ \kappa_{11} = 11.2 \times 10^{-9}\text{C}^2/\text{N m}^2, \kappa_{33} = 12.6 \times 10^{-9}\text{C}^2/\text{N m}^2, \\ \gamma_{11} = 5 \times 10^{-6}\text{Ns}^2/\text{C}^2, \gamma_{33} = 10 \times 10^{-6}\text{Ns}^2/\text{C}^2. \end{aligned} \quad (52)$$

$$\begin{aligned} \text{CoFe}_2\text{O}_4 : \\ c_{11} = 286\text{GPa}, c_{13} = 170\text{GPa}, c_{33} = 269.5\text{GPa}, \\ c_{44} = 45.3\text{GPa}, \kappa_{11} = 0.08 \times 10^{-9}\text{C}^2/\text{N m}^2, \\ \kappa_{33} = 0.093 \times 10^{-9}\text{C}^2/\text{N m}^2, h_{31} = 550\text{N/A m}, \\ h_{33} = 580.3\text{N/A m}, h_{15} = 699.7\text{N/A m}, \\ \gamma_{11} = 590 \times 10^{-6}\text{Ns}^2/\text{C}^2, \gamma_{33} = 157 \times 10^{-6}\text{Ns}^2/\text{C}^2. \end{aligned} \quad (53)$$

To verify the correctness of the displacement extrapolation formulae 32, 36 and 47 presented in the above sections, a special material combination of $V_f^I = V_f^{II} = 0.5$ is considered as the first example, which is theoretically equivalent to a central crack in a homogeneous MEE plate solved by Garcia-Sanchez et al. [25]. It should be pointed out that a tiny deviation of one constant should be given to avoid the numerical degeneration. In practice, $\gamma_{33} = 83.5001 \times 10^{-6} \text{ N s}^2/\text{C}^2$ for material II is in use. The field intensity factors are normalized by

$$\left\{ \begin{array}{l} K_I^* = K_I/K_0, K_{II}^* = K_{II}/K_0, \\ K_D^* = (e_{22}/\kappa_{22}) K_D/K_0, K_B^* = (h_{22}/\gamma_{22}) K_B/K_0 \end{array} \right. \quad (54)$$

with $K_0 = \sigma_{22}^\infty \sqrt{\pi a}$. To measure the intensity of the electromagnetic impacts, the following loading parameters

$$\lambda = (e_{22}/\kappa_{22}) D_2^\infty/\sigma_{22}^\infty, \Lambda = (h_{22}/\gamma_{22}) B_2^\infty/\sigma_{22}^\infty. \quad (55)$$

This bi-material system under the coupling loads of $\sigma_{22}^\infty = 1\text{MPa}$ and $\lambda = \Lambda = 1$ is solved by a dual boundary element method as proposed by Garcia-Sanchez et al. [25] together with a sub-domain technique. The field intensity factors are obtained by the formula 32. Meantime, this crack model is also analyzed by using the XFEM software as described in Bui and Zhang [30] and the fracture parameters are extracted via Eq. 47. For the clarity, only the results are presented and compared in Table 1. All the BEM and XFEM results are compared with the corresponding results for a homogenous crack problem via the relative errors. The errors of the field intensity factors are all less than 0.3% except K_{II}^* . Even the errors of K_{II}^* are also within 5%. They clearly show the correctness and accuracy of these extrapolation formulae.

Further, a real interface crack is considered for the case $V_f^I = 0.5$ and $V_f^{II} = 0.2$ in the following example. In this case, The oscillatory singularity for this material combination is real because of $\text{tr}[\mathbf{E}^2] > 0$. The same coupling loads as the first example, i.e., $\lambda = \Lambda = 1$, are considered. The BEM results by using Eq. 32 and the corresponding XFEM results via Eq. 47 are compared in Table 2. All the errors of the field intensity factors are within 3.5%. The correctness of the extrapolation formulae 32 and 47 are verified again.

Table 1: Fracture parameters of a MEE interface crack for $V_f^I = V_f^{II} = 0.5$

Fracture parameters	Homog. results	BEM results via Eq. 32	Error (%)	XFEM results via Eq. 47	Error (%)
K_I^*	1.065296	1.068288	0.28086	1.06816	0.26883
K_{II}^*	-0.012514	-0.012897	3.06304	-0.0129	3.0845
K_D^*	0.999712	1.002415	0.27037	1.002295	0.25835
K_B^*	0.918016	0.920544	0.27537	0.920434	0.26334

Table 2: Fracture parameters of a MEE interface crack for $V_f^I = 0.5$ and $V_f^{II} = 0.2$

Fracture parameters	BEM results via Eq. 32	XFEM results via Eq. 47	Error (%)
K_I^*	1.08846	1.08645	0.18467
K_{II}^*	-0.08803	-0.08504	3.39657
K_D^*	1.08186	1.07948	0.21999
K_B^*	1.07933	1.07755	0.16492

Acknowledgement: This work was supported by the Natural Science Foundation of China under Grant No. 11472021 and the Japan Society for the Promotion of Science (JSPS) under Grant No. 26-04055, which are gratefully acknowledged, additional thanks for Dr. Garcia-Sanchez's help.

References

- [1] Van Suchtelen J., Product properties: a new application of composite materials, *Phillips Res. Rep.*, **1972**, *27*, 28-37.
- [2] Nan C.W., Magnetolectric effect in composite of piezoelectric and piezomagnetic phases, *Phys. Rev. B*, **1994**, *50*, 6082-6088.
- [3] Hadjiloizi D.A., Kalamkarov A.L., Metti Ch., Georgiades A.V., Analysis of smart piezo-magneto-thermo-elastic composite and reinforced plates: Part I-model development, *Curved and Layered Structures*, **2014**, *1*, 11-31.
- [4] Hadjiloizi D.A., Kalamkarov A.L., Metti Ch., Georgiades A.V., Analysis of smart piezo-magneto-thermo-elastic composite and reinforced plates: Part II-applications, *Curved and Layered Structures*, **2014**, *1*, 32-58.
- [5] Ramirez F., Heyliger P.R., Pan E., Free vibration response of two-dimensional magneto-electro-elastic laminated plates, *Journal of Sound and Vibration*, **2006**, *292*, 626-644.
- [6] Razavi S., Shooshtari A., Nonlinear free vibration of magneto-electro-elastic rectangular plates, *Composite Structures*, **2015**, *119*, 377-384.
- [7] Xin L., Hu Z., Free vibration of simply supported and multilayered magneto-electro-elastic, *Composite Structures*, **2015**, *121*, 344-350.
- [8] Wang B.L., Mai Y.W., Crack tip field in piezoelectric/piezomagnetic media, *Eur. J. Mech. A/Solids*, **2003**, *22*, 591-602.
- [9] Hu K.Q., Li G.Q., Zhong Z., Fracture of a rectangular piezoelectromagnetic body, *Mech. Res. Commun.*, **2006**, *33*, 482-492.
- [10] Wang B.L., Mai Y.W., Fracture of piezoelectromagnetic materials, *Mech. Res. Commun.*, **2004**, *31*, 65-73.
- [11] Song Z.F., Sih G.C., Crack initiation behavior in magneto-electroelastic composite under in-plane deformation, *Theor. Appl. Frac. Mech.*, **2003**, *39*, 189-207.
- [12] Tian W.Y., Gabbert U., Multiple crack interaction problem in magneto-electroelastic solids, *Eur. J. Mech. A/Solids*, **2004**, *23*, 599-614.
- [13] Tian W.Y., Rajapakse R.K.N.D., Fracture analysis of magneto-electroelastic solids by using path independent integrals, *Int. J. Fract.*, **2005**, *131*, 311-335.
- [14] Wang B.L., Mai Y.W., Applicability of the crack-face electromagnetic boundary conditions for fracture of magneto-electroelastic materials, *Int. J. Solids Struct.*, **2007**, *44*, 387-398.
- [15] Niraula O.P., Wang B.L., A magneto-electro-elastic material with a penny-shaped crack subjected to temperature loading, *Acta Mech.*, **2006**, *187*, 151-168.
- [16] Zhao M.H., Yang F., Liu T., Analysis of a penny-shaped crack in a magneto-electro-elastic medium, *Philos. Mag.*, **2006**, *86*, 4397-4416.
- [17] Li R., Kardomateas G.A., The mode III interface crack in piezo-electro-magneto-elastic dissimilar bimaterials, *J. Appl. Mech.*, **2006**, *73*, 220-227.
- [18] Rogowski B., Exact solution for an anti-plane interface crack between two dissimilar magneto-electro-elastic half-spaces, *Smart Mater. Research*, **2012**, *78*, 6190.
- [19] Su R.K.L., Feng W.J., Fracture behavior of a bonded magneto-electro-elastic rectangular plate with an interface crack, *Arch. Appl. Mech.*, **2008**, *78*, 343-362.
- [20] Wang B.L., Mai Y.W., Closed-form solution for an antiplane interface crack between two dissimilar magneto-electroelastic layers, *J. Appl. Mech.*, **2006**, *73*, 281-290.
- [21] Feng W.J., Li Y.S., Xu Z.H., Transient response of an interfacial crack between dissimilar magneto-electroelastic layers under magneto-electromechanical impact loadings, Mode-I problem, *Int. J. Solids Struct.*, **2009**, *46*, 3346-3356.
- [22] Wang B.L., Mai Y.W., Self-consistent analysis of coupled magneto-electroelastic fracture. Theoretical investigation and finite el-

- ement verification, *Comput. Methods Appl. Mech. Engrg.*, **2007**, *196*, 2044-2054.
- [23] Rojas-Díaz R., Sukumar N., Sáez A., García-Sánchez F., Fracture in magnetoelastoelectric materials using the extended finite element method, *Int. J. Numer. Meth. Engrg.*, **2011**, *88*, 1238-1259.
- [24] Sladek J., Sladek V., Sulek P., Pan E., Fracture analysis of cracks in magneto-electro-elastic solids by the MLPG, *Comput. Mech.*, **2008**, *42*, 697-714.
- [25] García-Sánchez F., Rojas-Díaz R., Saez A., Zhang Ch., Fracture of magnetoelastoelectric composite materials using boundary element method (BEM), *Theor. Appl. Fract. Mech.*, **2007**, *47*, 192-204.
- [26] Wünsche M., Sáez A., García-Sánchez F., Zhang Ch., Transient dynamic crack analysis in linear magnetoelastoelectric solids by a hypersingular time-domain BEM, *Eur. J. Mech. A/Solids*, **2012**, *32*, 118-130.
- [27] Huang G.Y., Wang B.L., Mai Y.W., Effect of Interfacial Cracks on the Effective Properties of Magnetoelastoelectric Composites. *J. Intel. Mat. Syst. Str.*, **2009**, *20*, 963-968.
- [28] Lei, J., Garcia-Sanchez F., Zhang Ch., Determination of dynamic intensity factors and time-domain BEM for interfacial cracks in anisotropic piezoelectric materials, *Int. J. Solids Struct.*, **2013**, *50*, 1482-1493.
- [29] Lei J., Zhang Ch., On the generalized Barnett-Lothe tensors for anisotropic magnetoelastoelectric materials, *Eur. J. Mech. A/Solids*, **2014**, *46*, 12-21.
- [30] Bui Q.T., Zhang Ch., Analysis of generalized dynamic intensity factors in cracked magneto-electroelastic solids by the XFEM, *Finite Elem. Anal. Des.*, **2013**, *69*, 19-36.
- [31] Li Y., Viola E., Size effect investigation of a central interface crack between two bonded dissimilar materials, *Composite Structures*, **2013**, *105*, 90-107.
- [32] Viola E., Tornabene F., Ferretti E., Fantuzzi N., GDQFEM numerical simulations of continuous media with cracks and discontinuities. *CMES-Comp. Model. Eng.*, **2013**, *94(4)*, 331-369.